

# STABLE CARBON AND NITROGEN ISOTOPE RATIO IN $PM_{10}$ AND SIZE SEGREGATED AEROSOL PARTICLES OVER THE BALTIC SEA

I. Garbarienė<sup>a</sup>, V. Remeikis<sup>b</sup>, A. Mašalaitė<sup>b</sup>, A. Garbaras<sup>b</sup>, T. Petelski<sup>c</sup>,

P. Makuch<sup>c</sup>, and U. Dusek<sup>d</sup>

<sup>a</sup>Department of Environmental Research, Center for Physical Sciences and Technology, Savanorių 231, 02300 Vilnius, Lithuania

<sup>b</sup>Department of Nuclear Research, Center for Physical Sciences and Technology, Savanorių 231, 02300 Vilnius, Lithuania

<sup>c</sup>Physical Oceanography Department, Institute of Oceanology PAS, Powstańców Warszawy 55, PL-81-712 Sopot, Poland

<sup>d</sup>Centre for Isotope Research (CIO), University of Groningen, Groningen, The Netherlands

Email: inga.garbariene@ftmc.lt

Received 22 May 2019; revised 25 July 2019; accepted 30 September 2019

We analysed  $\delta^{13}C$  of total carbon (TC) and  $\delta^{15}N$  of total nitrogen (TN) in submicron ( $PM_{10}$ ) and size segregated aerosol particles ( $PM_{0.056-2.5}$ ) collected during a cruise in the Baltic Sea from 9 to 17 November 2012.

$PM_{10}$  were characterized by the highest  $\delta^{13}C$  (–26.4‰) and lowest  $\delta^{15}N$  (–0.2 and 0.8‰) values when air masses arrived from the southwest direction (Poland). The obtained  $\delta^{13}C$  values indicated that combined emissions of coal and diesel/gasoline combustion were the most likely sources of TC. The depleted  $\delta^{15}N$  values indicated that TN originated mainly from liquid fuel combustion (road traffic, shipping) during this period. The lowest  $\delta^{13}C$  and highest  $\delta^{15}N$  values were determined in  $PM_{10}$  samples during the western airflow when the air masses had no recent contact with land. The highest  $\delta^{15}N$  values were probably associated with chemical aging of nitrogenous species during long-range transport, the lowest  $\delta^{13}C$  values could be related to emissions from diesel/gasoline combustion, potentially from ship traffic.

The  $\delta^{13}C$  analysis of size-segregated aerosol particles  $PM_{0.056-2.5}$  revealed that the lowest  $\delta^{13}C$  values were observed in the size range from 0.056 to 0.18  $\mu m$  and gradual  $^{13}C$  enrichment occurred in the size range from 0.18 to 2.5  $\mu m$  due to different sources or formation mechanisms of the aerosols.

**Keywords:**  $PM_{10}$  and  $PM_{0.056-2.5}$ , stable carbon and nitrogen isotope ratios, source apportionment, southeastern Baltic Sea region

**PACS:** 92.60.Mt, 92.60.Sz, 92.60.hf

## 1. Introduction

The coastal environment is a special environment where the mixing of marine boundary and continental boundary layers occurs [1, 2] and it is influenced by both marine and continental sources. Carbonaceous material accounts for a significant fraction of both marine and continental aerosols [3–5]. The coastal marine atmosphere adjacent to large urban and industrial centres can be strongly impacted by pollution emissions, result-

ing in high loading of pollutants in the ambient air. According to several authors, the carbonaceous aerosol concentration in European coastal areas, including the coastal region of the Baltic Sea, exceeds typical clean marine concentrations of 0.14–0.6  $\mu g/m^3$  and nearly reaches the values of urban particle concentrations of 5–10  $\mu g/m^3$  [6]. A substantial influence of continental emissions has been widely observed, not only in the coastal areas but also in the open seas [7, 8]. In addition to emissions originated from the oceans,

continental outflow is also an important source of carbonaceous aerosols in marine environment [3, 9, 10]. Chesselet et al. (1981) [11] concluded that more than 80% of atmospheric particulate organic carbon was of continental origin over remote marine areas. Fu et al. (2011) [9] reported that fossil fuel combustion and biomass burning are the major sources of organic aerosols over the Western Pacific. Marine natural emissions of carbonaceous aerosol (biological sources) were found to be the most important contributor only over some remote oceanic areas [3, 4]. Anthropogenic carbonaceous aerosols mainly originate from fuel combustion, industrial processes and biomass/biofuel burning. Due to a complex mixture of the marine and continental air masses source, the apportionment of the carbonaceous fraction is especially difficult in the coastal environment.

The stable carbon isotope ratio ( $\delta^{13}\text{C}$ ) of carbonaceous aerosol was used in a number of studies to identify and apportion main pollution sources [12–18]. The stable carbon isotope ratio was also used to quantify aerosol particles of marine origin [19, 20].

Nitrogen isotope analysis is also a useful tool to discriminate the origin of nitrogen containing aerosol particles, but less used than  $\delta^{13}\text{C}$ , because  $\delta^{15}\text{N}$  depends on the sources of PM and can also be modified by chemical and physical processes in the atmosphere [21–25]. Particulate matter derived from biomass burning (C3 plants) had  $\delta^{15}\text{N}$  values ranging from 2 to 19.5‰ [26]. Widory (2007) [21] determined  $\delta^{15}\text{N}$  values for the main heating sources such as natural gas  $7.7 \pm 5.9\text{‰}$ , coal combustion  $-5.6\text{‰}$  and fuel oil  $-7.5 \pm 8.3\text{‰}$ . Traffic related PM had  $\delta^{15}\text{N}$  values about  $4.6 \pm 0.8\text{‰}$  [21]. Total nitrogen (TN) in aerosol particles is the sum of ammonium ( $\text{NH}_4^+$ ), nitrate ( $\text{NO}_3^-$ ) and organic nitrogen (ON). These forms of nitrogen have different sources and transformation pathways in the atmosphere, resulting in different  $\delta^{15}\text{N}$  values of TN [27–31]. Previous authors demonstrated that using a combination of stable carbon and stable nitrogen isotopic compositions (in  $\text{NH}_4^+$ ,  $\text{NO}_3^-$  and ON) facilitates the study of the contribution of anthropogenic (biomass burning and fossil fuel) and biogenic (marine) sources and chemical aging to ambient aerosol [32, 33].

The major goal of this study was to gain an insight into the origin of carbon and nitrogen in submicron and size-segregated aerosol particles

in the coastal environment and characterize the advection of continental pollution to the marine environment using TC and TN isotopic analysis.

## 2. Materials and methods

Aerosol samples were collected over the Baltic Sea during a cruise from 9 to 17 November 2012.  $\text{PM}_{10}$  samples were collected at a flow rate of 30 L/min using a low volume sampler (Leckel). Five  $\text{PM}_{10}$  samples were collected during the cruise on quartz fiber filters (Millipore). In addition, size segregated aerosol samples were collected with a Micro-Orifice Uniform Deposit Impactor (MOUDI) model 110 with a flow rate of 30 L/min, and 50% aerodynamic cutoff diameters of 11 stages of 18, 9.9, 6.2, 2.5, 1.8, 1.0, 0.56, 0.32, 0.18, 0.10 and 0.056  $\mu\text{m}$ . Aluminum foil was used as an impaction surface. The quartz filters were pre-combusted at 600°C for 24 h to remove organic contaminants. After sampling all aerosol samples were stored in a refrigerator.

Figure 1 shows the cruise tracks which are indicated by sample ID from F1 to F5. The meteorological conditions, sampling periods and air mass back trajectory directions are presented in Table 1.

All aerosol samples were analysed for TC and TN contents and their isotopic compositions using an elemental analyzer (EA) FlashEA 1112 connected to a stable isotope ratio mass spectrometer (IRMS) ThermoFinnigan Delta Plus Advantage by the method described in [34, 35]. Caffeine (IAEA-600)

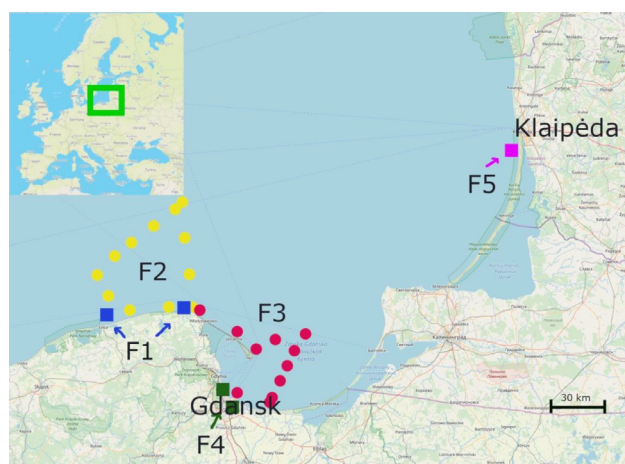


Fig. 1. Map of the cruise track and sampling sites. Sample IDs F1, F2, F3, F4 and F5 indicate the ship position during the sample collection.

Table 1. Data about the samples (PM<sub>1</sub> and MOUDI) and weather conditions during the cruises in the Baltic Sea on 9–17 November 2012. See Fig. 1, coloured online.

Ship track colour	Sample ID	Date of measurements	T, °C	RH, %	Wind speed, m/s	Wind direction, °	Air mass backward trajectories	Ship location
PM1 samples								
Blue track	F1	09–11.11.2012	8	77	4–13 (8.4)	120–180	S–W	Near coastline of Poland
Yellow track	F2	11–12.11.2012	8	83	3.5–12.5 (7.4)	230–260	W	Baltic Sea
Red track	F3	12–14.11.2012	6	80	2.5–8.5 (5)	230–270	W	Near coastline of Poland and Baltic Sea
Green track	F4	14–15.11.2012	5	7	3.5–10 (7)	210–240	S–W	Near harbour (Gdansk)
Pink track	F5	15–17.11.2012	6	83	4–9 (6.6)	170–250	S, W–NW	Route: Gdansk–Klaipėda
MOUDI samples								
Blue, yellow and red tracks	M1	09–13.11.2012	7.5	80	2.5–13 (7.5)	120–270	S, W (west prevailing)	Near coastline of Poland and Baltic Sea
Green and pink tracks	M2	13–17.11.2012	5.3	82	2.5–10 (6.2)	170–250	S, W	Near harbours (Gdansk, Klaipėda)

was used as a secondary reference material to determine TC, TN, and their isotopic compositions ( $\delta^{13}\text{C}$  and  $\delta^{15}\text{N}$ ).

Meteorological parameters recorded at a meteorological synoptic station at shipboard during the cruise include ambient temperature, relative humidity, wind speed and wind direction. The average ambient temperature was 7°C ranging from 3 to 10°C. The minimum air temperature was reported on 14–15 November 2012, while the maximum one on 9–12 November (see Table 1). The daily average relative humidity ranged from 64 to 88% (average 83%). The local wind direction varied between 120 to 280° and the average wind speed was 6.5 m/s.

Backward trajectories were calculated using the hybrid single particle Lagrangian (HYSPLIT) model from the National Oceanic and Atmospheric Administration (NOAA) [36]. The trajectories were calculated every 6 h with a total 72 h duration at 500 m AGL (Above Ground Level). The analysis of air mass back trajectories indicates that during the sampling period S, SW and W air masses were prevailing (Fig. 2).

### 3. Results

#### 3.1. Concentrations of total carbon and total nitrogen in PM<sub>1</sub>

The variations of TC and TN mass concentration measured aboard RV *Oceania* during the cruise on the Baltic Sea are shown in Fig. 3. TC concentrations ranged from 1.95 to 5.91  $\mu\text{g}/\text{m}^3$  (average  $4.27 \pm 1.56 \mu\text{g}/\text{m}^3$ ). TN concentrations varied from 1.3 to 2.8  $\mu\text{g}/\text{m}^3$  (average  $2.4 \pm 0.8 \mu\text{g}/\text{m}^3$ ). As shown in Fig. 3, the TN concentration followed the TC concentration which could point to the same aerosol sources or source regions. The TN and TC concentrations depended on the ship location and on the air mass origin during the sampling campaign. The highest concentrations of TC (average  $5.3 \pm 0.6 \mu\text{g}/\text{m}^3$ ) and TN (average  $2.8 \pm 0.8 \mu\text{g}/\text{m}^3$ ) were measured when southern and southwestern air masses from Poland, Germany and the Czech Republic and the southern wind from Poland were prevailing (F1, F4, F5). These findings suggest that the majority of TC and TN in PM<sub>1</sub> were derived from regional anthropogenic sources during these time periods.

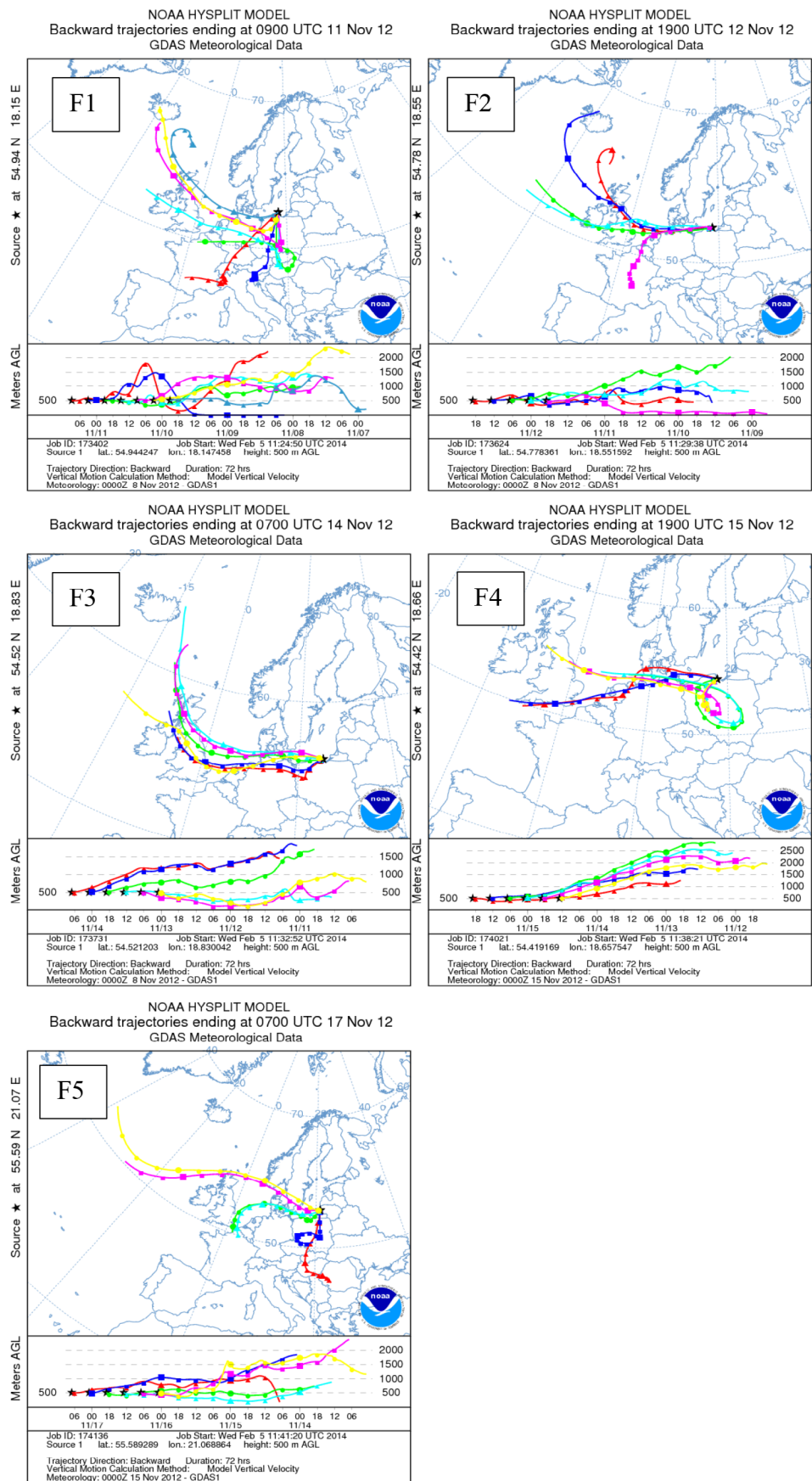


Fig. 2. Air mass backward trajectories during a cruise in the Baltic Sea from 9 to 17 November, 2012.

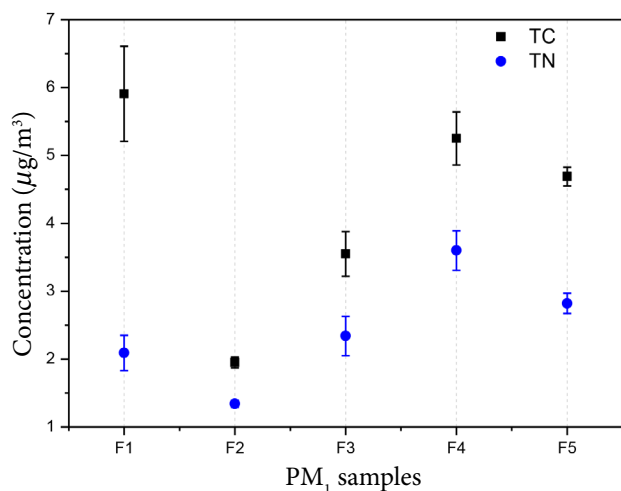


Fig. 3. TC and TN concentration of  $PM_1$  fraction.

The lowest TC and TN concentrations (F2, F3) were observed in the western outflow when air masses generally came from the North Atlantic, but passed over the industrial regions of England. The observed TN and TC concentrations were higher than those reported for ‘clean marine’ aerosol (TC about  $0.1\text{--}0.5 \mu\text{g}/\text{m}^3$ , TN about  $0.02\text{--}0.03 \mu\text{g}/\text{m}^3$ ) at Mace Head in the North Atlantic [19, 37, 38]. Previous studies showed that carbonaceous aerosol particles carried to the coastal site of the Baltic Sea (Preila) from the northwestern direction via England were affected by anthropogenic sources (continental and marine transport) rather than biogenic sources (marine) [39, 40]. Ceburnis et al. (2011) [19] revealed that in clean marine air masses (which had no continental pathways) 8–20% of carbonaceous aerosol could be attributed to fossil fuel sources (e.g. shipping). The area of our study, namely, the Baltic Sea, is one of the busiest seas in the world (>2,000 ships per day) and the amount of maritime traffic is predicted to keep growing (<http://www.helcom.fi>). The modelling results have shown that the relative contribution of ship emissions to the annual mean  $\text{NO}_2$  is more than 40% over the Baltic Sea and 22–28% for the entire Baltic Sea region. The average contributions of ships to the levels of  $PM_{2.5}$  and EC (elemental carbon) are in a range of 4.3–6.5% and 5–7%, respectively [41].

The sample with the lowest total carbon concentration F2 (TC =  $1.95 \pm 0.08 \mu\text{g}/\text{m}^3$ , TN =  $1.34 \pm 0.05 \mu\text{g}/\text{m}^3$ ) was obtained when the ship was located about 30–40 km from the northern part of the Polish coast and the westerly wind direction was pre-

vailing. This sample was most likely influenced by long-range transport (anthropogenic) and marine (biogenic and shipping) sources, rather than regional coastal sources. However, we assume that due to a low sea biological activity in the late fall period (9–17 November 2012) the contributions from marine biogenic sources to samples F1–F5 were insignificant. During the relatively clean western air mass period (F3) the concentrations of TC ( $3.55 \pm 0.33 \mu\text{g}/\text{m}^3$ ) and TN ( $2.34 \pm 0.29 \mu\text{g}/\text{m}^3$ ) notably increased compared to those of sample F2. This happens when the ship spends more time nearby the coastline of Poland. Thus, sample F3 was influenced by both long-range transport and regional coastal land-based pollution sources. Relatively high concentrations of TC and TN together with the back trajectory analysis suggest that  $PM_1$  samples during this study were affected by anthropogenic regional sources and long-range transport.

### 3.2. Carbon and nitrogen isotopic composition of $PM_1$

The analysis of  $\delta^{13}\text{C}$ -TC and  $\delta^{15}\text{N}$ -TN can give an indication of the origin of carbonaceous and nitrogen species in  $PM_1$ .  $\delta^{13}\text{C}$ -TC of  $PM_1$  varied from  $-27.5$  to  $-26.2\text{‰}$  with an average of  $-26.8 \pm 0.5\text{‰}$ . The mean  $\delta^{13}\text{C}$  observed over the Baltic Sea is comparable to that determined in several urban and anthropogenically influenced locations in Europe [16, 17, 42, 43]. The minimum  $\delta^{13}\text{C}$  value ( $-27.5 \pm 0.2\text{‰}$ ) was observed on 11–12 November (F2) when the lowest TC concentration and the western outflow was prevailing (Fig. 4). Higher  $\delta^{13}\text{C}$  ( $-26.6 \pm 0.4\text{‰}$ ) values were registered in the  $PM_1$  samples with higher TC concentrations (F1, F3, F4) when the ship was located near the coastline of Poland and the highest  $\delta^{13}\text{C}$  value was observed in F5 near the harbour of Klaipėda. It seems that continental sources responsible for higher carbon concentrations are associated with higher  $\delta^{13}\text{C}$  values. The variation (from  $-27.0$  to  $-26.2\text{‰}$ ) in these samples indicated consistent regional coastal sources.

A wide variation of the total nitrogen isotopic ratios of  $PM_1$  (from  $-0.2$  to  $10\text{‰}$ ) was observed during the study period (Fig. 4). The mean of  $\delta^{15}\text{N}$  in  $PM_1$  shows larger variations than those in  $\delta^{13}\text{C}$ . These variations of  $\delta^{15}\text{N}$ -TN may be due to the changes in the contribution of regional pollution sources, chemical aging of nitrogen species and

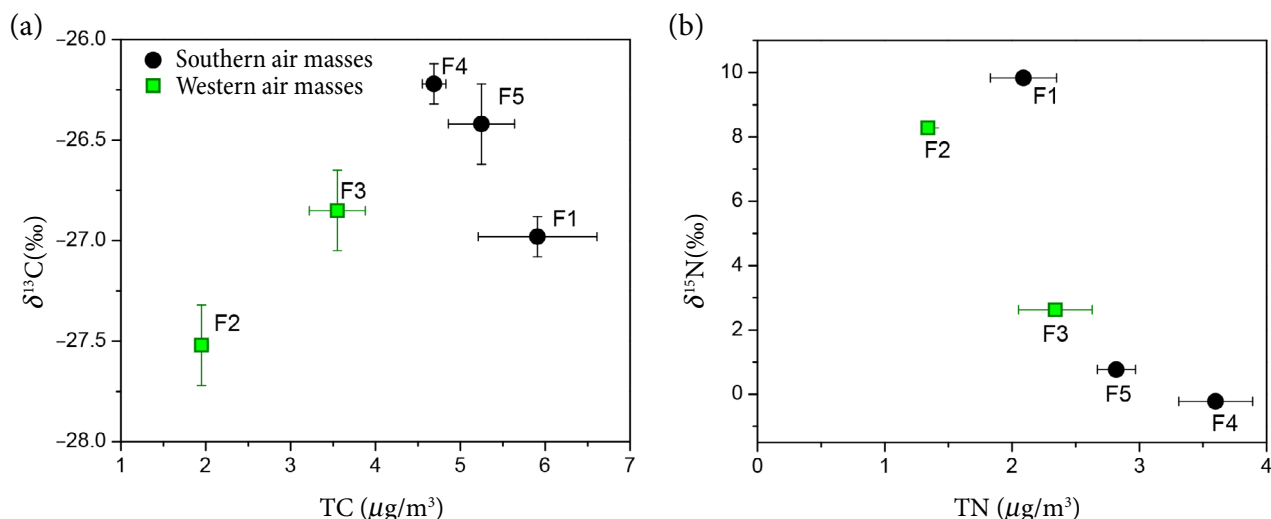


Fig. 4. Relationships between (a) TC concentrations and stable carbon isotopes, (b) TN concentrations and stable nitrogen isotopes.

abundances of  $\text{NH}_4^+$  and  $\text{NO}_3^-$  in TN 33]. A scatter plot of  $\delta^{15}\text{N}$  against TN in Fig. 4 shows a tendency towards depletion in  $^{15}\text{N}$  at higher TN concentrations, that was probably affected by a significant anthropogenic input from fossil fuel combustion which are generally depleted in  $^{15}\text{N}$  ( $\delta^{15}\text{N} < 0$ ) [21] compared to other sources.

Figure 5 shows that  $\delta^{13}\text{C}$  is anti-correlated with  $\delta^{15}\text{N}$  values during the campaign. The highest  $\delta^{13}\text{C}$  ( $-26.4\text{‰}$ ) and lowest  $\delta^{15}\text{N}$  ( $-0.2$  and  $0.8\text{‰}$ ) values were registered in samples F4 and F5 when air masses arrived mainly from the southwest direction (Poland). In this region, aerosol particles enriched in  $^{13}\text{C}$  are expected due to high contributions

of particles from coal combustion [13]. According to the official Polish Government Energy Policy Strategy, 89% of heat in Poland is generated from coal (<https://www.worldenergy.org>; <https://euracoal.eu>, 2018). Górká et al. (2014) [43] found that during the heating season in Poland coal-derived aerosol particles ( $\delta^{13}\text{C} = -24.5 \pm 0.5\text{‰}$ ) comprise about 40% of the elemental carbon fraction. Previous studies revealed that traffic-derived aerosol particles in Eastern European countries (Lithuania, Poland) typically have the mean  $\delta^{13}\text{C}$  signature of  $-28 \pm 0.5\text{‰}$  [13, 18, 44]. Relying on the carbon isotopic composition, we can conclude that possible sources of  $\text{PM}_{10}$  over the coastal areas were

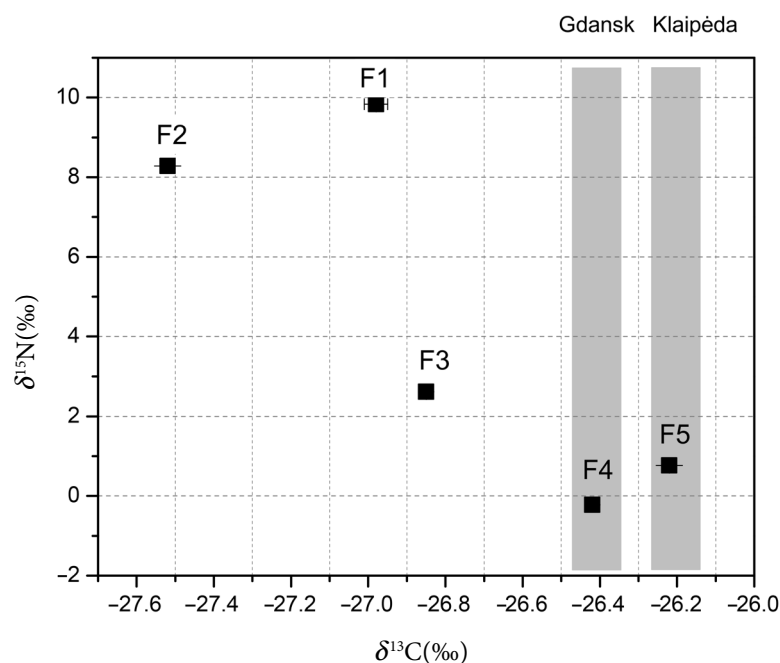


Fig. 5. Stable carbon isotope composition via nitrogen isotopic composition in the samples of  $\text{PM}_{10}$  fraction.

combined emissions of solid fuel (coal) burning and vehicle exhaust. Furthermore,  $^{13}\text{C}$  enriched  $\text{PM}_1$  samples in air masses from Poland are associated with higher contributions from coal combustion. The  $\delta^{13}\text{C}$  value for F2 is consistent with liquid fossil fuel combustion as the main source.

The lowest  $\delta^{15}\text{N}$  values (from  $-0.2$  to  $0.8\text{‰}$ ) together with the elevated TN concentration were observed on 14–17 November (samples F4, F5). Lower  $\delta^{15}\text{N}$  values indicate a significant impact from fuel oil and coal combustion [21]. However, coal combustion yields particles low in nitrogen content ( $0.33\%$ ). The nitrogen concentration in samples F4 and F5 was high and this suggests strong contributions of secondary nitrate. Vodička et al. (2019) [33] showed that a decrease in  $\delta^{15}\text{N}$  of TN was associated with a higher content of  $\text{NO}_3^-$ , and elevated  $\delta^{15}\text{N}$  values were caused by higher levels of  $\text{NH}_4^+$  or OrgN.  $\text{NO}_3^-$  originates mainly from fossil fuel combustion and biomass burning [45], while  $\text{NH}_4^+$  originates from agricultural activities, biological emissions and, to a minor extent, from anthropogenic combustion sources (fossil fuel and biomass burning) [46–50]. Heaton et al. (1991) [51] reported that  $\delta^{15}\text{N}$  of  $\text{NO}_x$  derived from diesel engines ranged from  $-13$  to  $-2\text{‰}$ , while those from coal-fired power stations ranged from  $6$  to  $13\text{‰}$ . Changes in the  $\delta^{15}\text{N}$  values during conversion of  $\text{NO}_x$  to nitrate are minor, therefore  $\delta^{15}\text{N}$  values of particulate nitrate imply  $\text{NO}_x$  sources [21, 52]. It has been reported by other authors that the transformation of  $\text{NO}_x$  to atmospheric nitrates elevates  $\delta^{15}\text{N}$  values (by about  $10$ – $15\text{‰}$ ) from the initial  $\delta^{15}\text{N}$  values of the  $\text{NO}_x$  sources [53]. We assume that  $\text{NO}_3^-$  was more abundant in samples F4 and F5 when the ship was close to a nearby harbour (Gdansk) and the conversion of  $\text{NO}_x$  to  $\text{NO}_3^-$  was more likely to be responsible for the observed  $\delta^{15}\text{N}$  of TN rather than the conversion of  $\text{NH}_3 \leftrightarrow \text{NH}_4^+$ . Bearing in mind the nitrogen oxides as a source of nitrogen in the aerosol particles we assume that  $\delta^{15}\text{N}$  values (from  $-0.2$  to  $0.8\text{‰}$ ) of samples F4 and F5 are similar to those of  $\text{NO}_x$  generated from vehicular exhaust or ship emissions. We can conclude that the dominant sources of TN in samples F4, F5 most probably reflect the  $\text{NO}_x$  input generated by liquid fuel combustion (on road traffic, shipping).

The highest  $\delta^{15}\text{N}$  values (up to  $10\text{‰}$ ) were observed on 9–12 November (F1, F2) and were ac-

companied by lower TN concentrations. High  $\delta^{15}\text{N}$  values imply that secondary formation of  $\text{NH}_4^+$  played a larger role in nitrogen contents of  $\text{PM}_1$  in these samples. Previous studies based on chemical analysis and the  $\delta^{15}\text{N}(\text{NH}_4^+)$  approach showed that in Poland fossil fuel burning is the main source of  $\text{NH}_4^+$  in precipitation during the heating season [54]. Precipitation samples during November are characterized by a low  $\text{NH}_4^+$  concentration and  $\delta^{15}\text{N}(\text{NH}_4^+)$  values in a range of  $5$ – $10\text{‰}$ . However, it is also possible that  $\delta^{15}\text{N}$  values have become more enriched during long-range transport to the site.

As shown in Fig. 5, samples F1, F2 are characterized by lower  $\delta^{13}\text{C}$  ( $-27.0\text{‰}$  and  $27.5\text{‰}$ , respectively) and the highest  $\delta^{15}\text{N}$  ( $9.8 \pm 0.1\text{‰}$  and  $8.3 \pm 0.2\text{‰}$ , respectively) values. The  $\delta^{13}\text{C}$  values for samples F1, F2 imply that they were much less affected by coal, but more by diesel/gasoline combustion (shipping and traffic).

Combining stable carbon and nitrogen isotopic data with the TN and TC concentrations we were able to discriminate likely aerosol sources. Relatively high  $\delta^{13}\text{C}$  and low  $\delta^{15}\text{N}$  values indicate fossil fuel (coal and diesel) as a dominant source for the aerosol particles consistent with air mass back trajectories crossing Poland, while relatively low  $\delta^{13}\text{C}$  and high  $\delta^{15}\text{N}$  values indicate that the main source of TC and TN could be shipping activities and aged aerosol particles, respectively.

### 3.3. $\delta^{13}\text{C}$ and $\delta^{15}\text{N}$ in size segregated aerosol particles

The total carbon and total nitrogen size distributions obtained from two MOUDI sampling periods (M1 9–13 November and M2 13–17 November) are presented in Fig. 6. During the M1 period (9–13 November) air masses were mainly transported from the western direction via the North Atlantic and England and only partly passed over southwestern Europe's industrial regions (Poland, Germany, the Czech Republic). This period is characterized as a relatively clean period. During the M2 period air masses were mainly passing over Southern Europe (polluted period).

As shown in Fig. 6, the size distributions of TC for relatively clean and polluted periods were different. During the cleaner period, TC exhibited bimodal mass-size distribution with the first

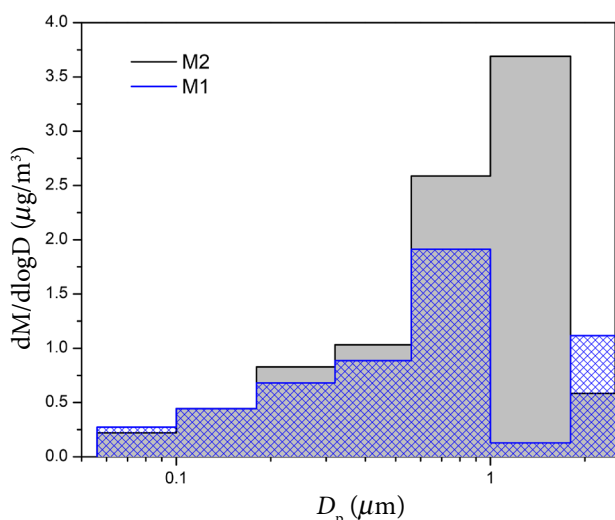


Fig. 6. The mass size distribution of TC in (a) relatively clean M1 and (b) polluted M2 periods.

peak clearly identified in the accumulation mode between 0.56 and 1  $\mu\text{m}$  and other slight and less-marked peak centered at approximately 1.8–2.5  $\mu\text{m}$ . During the polluted period, the shape of the TC size distribution had a unimodal peak in a size range of 1–1.8  $\mu\text{m}$ .

Figure 7 gives an overview of a stable carbon and nitrogen isotopic composition in size segregated aerosol particles. The stable carbon isotopic composition varied from  $-26.3 \pm 0.1\text{‰}$  to  $-28.2 \pm 0.1\text{‰}$  during the M1 period and from  $-25.2 \pm 0.2\text{‰}$  to  $-27.9 \pm 0.1\text{‰}$  during the M2 period. The first period M1 was characterized by a lower TC concentration and a lower variability

of  $\delta^{13}\text{C}$  values (1.9‰). During the polluted period M2 the highest TC concentration and a larger variability of  $\delta^{13}\text{C}$  values (2.7‰) were observed. The  $\delta^{13}\text{C}$  values had a similar distribution within the particle size during the relatively clean M1 and polluted M2 periods: the  $\delta^{13}\text{C}$  values increased with an increase of the size of fine particles. Most  $^{13}\text{C}$  depleted aerosol particles were observed in the size range from 0.056 to 0.18  $\mu\text{m}$ . The mean  $\delta^{13}\text{C}$  value in  $\text{PM}_{0.056-0.18}$  was  $-28.05 \pm 0.12\text{‰}$ , equivalent to  $\delta^{13}\text{C}$  values for vehicular exhaust ( $-28.0 \pm 0.9\text{‰}$ ) [13, 18]. These ultra-fine particles have typically short lifetimes and therefore are characteristic of local sources. We can conclude that local coastal sources are, therefore, mainly liquid fuel combustion. The observed  $\delta^{13}\text{C}$  values of  $\text{PM}_{0.18-2.5}$  ( $-26.4 \pm 0.1\text{‰}$ ) are a possible mixture of coal and diesel/gasoline combustion particles. Particles in this size range have longer lifetimes and can be transported from further distances, which explains the stronger influence of coal combustion. Moreover, the carbonaceous species during the M2 period were only slightly enriched in  $^{13}\text{C}$  ( $0.5 \pm 0.1\text{‰}$ ) compared to M1, suggesting similar sources for TC during both the periods. Nevertheless, higher  $\delta^{13}\text{C}$  values during the polluted period M2 point to a larger proportion of particles from coal combustion.

$\delta^{15}\text{N}$  shows a strong enrichment of  $^{15}\text{N}$  during the M1 period ( $\delta^{15}\text{N}$  about 11.5‰) in comparison with the M2 period ( $\delta^{15}\text{N}$  about 2.9‰). As

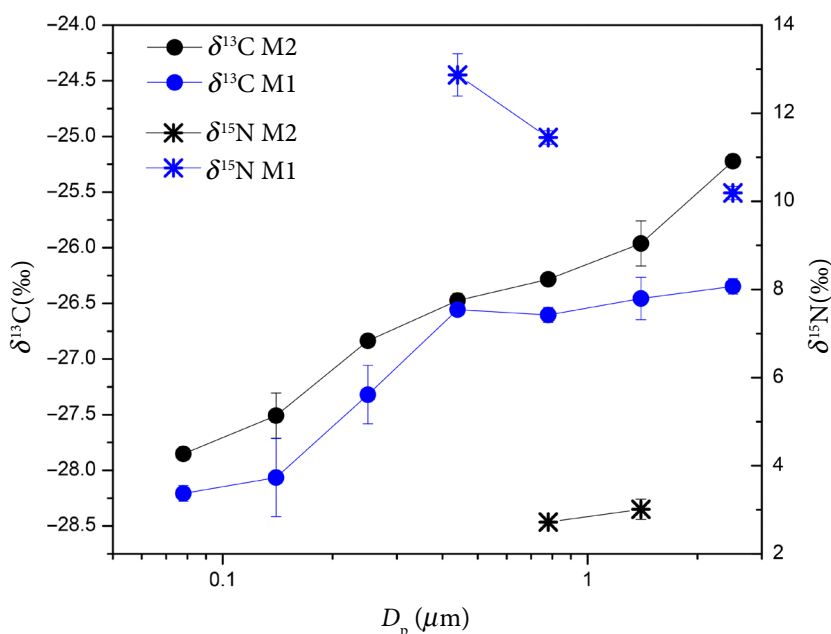


Fig. 7. Stable carbon and nitrogen isotopic composition in size segregated aerosol particles.

mentioned above (Subsection 3.2), in relatively clean air masses (M1) chemical aging of nitrogen species including the gas-to-particle exchange ( $\text{NH}_3 \leftrightarrow \text{NH}_4^+$ ) reaction during long-range transport can cause an enrichment of  $^{15}\text{N}$ . Possibly, higher  $\delta^{15}\text{N}$  values during the M1 period could also be attributed to the impact from biomass burning ( $\delta^{15}\text{N} = 10\text{--}20\text{‰}$ ). Fossil fuel combustion (traffic or ship emissions) was presumably the dominant source of aerosol nitrogen during the polluted period ( $\delta^{15}\text{N}$  about  $2.9\text{‰}$ ). During this period biomass burning sources are less likely, because  $\delta^{15}\text{N}$ -TN were depleted in  $^{15}\text{N}$ .

## Conclusions

Stable carbon and stable nitrogen isotope measurements were performed on  $\text{PM}_{10}$  and size resolved aerosol samples collected during the cruise in the Baltic Sea from 9 to 17 November 2012. Total carbon (TC) and total nitrogen (TN) concentrations varied from  $1.95$  to  $5.91 \mu\text{g}/\text{m}^3$  and from  $1.3$  to  $2.8 \mu\text{g}/\text{m}^3$ , respectively. Temporal variation of TC and TN concentrations during the campaign depended on the ship location and air mass origin. The back trajectory analysis suggests that relatively high TC and TN loadings are associated with continental air masses (S, SW) and indicates that  $\text{PM}_{10}$  samples are influenced by anthropogenic pollution. The total carbon isotopic composition of  $\text{PM}_{10}$  varied from  $-27.5$  to  $-26.2\text{‰}$  with an average of  $-26.8 \pm 0.5\text{‰}$ . The minimum  $\delta^{13}\text{C}$  value ( $-27.5 \pm 0.2\text{‰}$ ) was observed in  $\text{PM}_{10}$  samples with the lowest TC concentration when the western air masses were prevailing and the air mass did not have a recent contact with land. Higher  $\delta^{13}\text{C}$  ( $-26.6 \pm 0.4\text{‰}$ ) values were associated with the highest TC levels when the ship was located nearby the coastline of Poland and the air mass came from the south.

Based on the  $\delta^{13}\text{C}$  analysis of TC we conclude that combined emissions of solid fuel (coal) and diesel/gasoline combustion (vehicular exhaust/shipping) were the most possible sources of  $\text{PM}_{10}$  during continental outflow.

A wide variation of the total nitrogen isotopic ratios of  $\text{PM}_{10}$  (from  $-0.2$  to  $10\text{‰}$ ) was observed during the study period. Lower  $\delta^{15}\text{N}$  values indicated a significant influence from fossil fuel combustion, including ship emission and traffic. The high

$\delta^{15}\text{N}$  implies that the secondary formation of  $\text{NH}_4^+$  played a certain role in nitrogen contents of  $\text{PM}_{10}$ .

The  $\delta^{13}\text{C}$  values of size segregated aerosol particles ( $\text{PM}_{0.056\text{--}2.5}$ ) increased with increase in the size of aerosol particles. Most  $^{13}\text{C}$  depleted ( $\delta^{13}\text{C} = -28.05 \pm 0.12\text{‰}$ ) aerosol particles were observed in the size range from  $0.056$  to  $0.18 \mu\text{m}$ , suggesting predominant diesel/gasoline combustion sources for the ultra-fine particles of local, coastal origin. The carbonaceous species during the polluted period were slightly  $^{13}\text{C}$  enriched ( $0.5 \pm 0.1\text{‰}$ ) compared to those during the relatively clean period (M1), suggesting similar sources for TC during both periods. The higher  $\delta^{13}\text{C}$  values obtained during the polluted period (M2) implied a slightly larger proportion from coal combustion consistent with the air mass transport mainly from the south. On the other hand,  $\delta^{15}\text{N}$  shows a strong enrichment of  $^{15}\text{N}$  during the M1 period ( $\delta^{15}\text{N}$  about  $11.5\text{‰}$ ) in comparison with that during the M2 period ( $\delta^{15}\text{N}$  about  $2.9\text{‰}$ ). The highest  $\delta^{15}\text{N}$  values imply that TN during a relatively clean period was significantly influenced by chemical aging of nitrogen species. The lower  $\delta^{15}\text{N}$  values ( $\delta^{15}\text{N}$  about  $2.9\text{‰}$ ) obtained during the polluted period indicate that fossil fuel sources were dominant.

In summary, the study of stable carbon and stable nitrogen isotopes provides useful information on different sources and production pathways of TC and TN in fine aerosol particles.

## References

- [1] F. Wang, Y. Chen, X. Meng, J. Fu, and B. Wang, The contribution of anthropogenic sources to the aerosols over East China Sea, *Atmos. Environ.* **127**, 22–33 (2016).
- [2] M. Kang, F. Yang, H. Ren, W. Zhao, Y. Zhao, L. Li, Y. Yan, Y. Zhang, S. Lai, Y. Zhang, et al., Influence of continental organic aerosols to the marine atmosphere over the East China Sea: Insights from lipids, PAHs and phthalates, *Sci. Total Environ.* **607–608**, 339–350 (2017).
- [3] C.D. O'Dowd and G.D. Leeuw, Marine aerosol production: A review of the current knowledge, *Philos. Trans. Royal Soc. A* **365**, 1753–1774 (2007).
- [4] C.D. O'Dowd, M.C. Facchini, F. Cavalli, D. Ceburnis, M. Mircea, S. Decesari, S. Fuzzi, Y.J. Yoon,

- and J.-P. Putaud, Biogenically driven organic contribution to marine aerosol, *Nature* **431**, 676–680 (2004).
- [5] J.-P. Putaud, F. Raes, R. Van Dingenen, E. Brüggemann, M.C. Facchini, S. Decesari, S. Fuzzi, R. Gehrig, C. Hüglin, P. Laj, et al., A European aerosol phenomenology-2: Chemical characteristics of particulate matter at kerbside, urban, rural and background sites in Europe, *Atmos. Environ.* **38**, 2579–2595 (2004).
- [6] A.U. Lewandowska, M. Bełdowska, A. Witkowska, L. Falkowska, and K. Wiśniewska, Mercury bonds with carbon (OC and EC) in small aerosols (PM<sub>1</sub>) in the urbanized coastal zone of the Gulf of Gdansk (southern Baltic), *Ecotoxicol. Environ. Saf.* **157**, 350–357 (2018).
- [7] B. Kunwar and K. Kawamura, One-year observations of carbonaceous and nitrogenous components and major ions in the aerosols from subtropical Okinawa Island, an outflow region of Asian dusts, *Atmos. Chem. Phys.* **14**, 1819–1836 (2014).
- [8] D. Shang, M. Hu, Q. Guo, Q. Zou, J. Zheng, and S. Guo, Effects of continental anthropogenic sources on organic aerosols in the coastal atmosphere of East China, *Environ. Pollut.* **229**, 350–361 (2017).
- [9] P. Fu, K. Kawamura, and K. Miura, Molecular characterization of marine organic aerosols collected during a round-the-world cruise, *J. Geophys. Res.* **116**, D13302 (2011).
- [10] Y. Zhao, Y. Zhang, P. Fu, S.S.H. Ho, K.F. Ho, F. Liu, S. Zou, S. Wang, and S. Lai, Non-polar organic compounds in marine aerosols over the northern South China Sea: Influence of continental outflow, *Chemosphere* **153**, 332–339 (2016).
- [11] R. Chesselet, M. Fontugne, P. Buat-Ménard, U. Ezat, and C.E. Lambert, The origin of particulate organic carbon in the marine atmosphere as indicated by its stable carbon isotopic composition, *Geophys. Res. Lett.* **8**, 345–348 (1981).
- [12] D. Widory, Combustibles, fuels and their combustion products: A view through carbon isotopes, *Combust. Theor. Model.* **10**, 831–841 (2006).
- [13] M. Górka and M.-O. Jędrysek,  $\delta^{13}\text{C}$  of organic atmospheric dust deposited in Wrocław (SW Poland): Critical remarks on the passive method, *Geol. Q.* **52**, 115–126 (2008).
- [14] E.N. Kirillova, R.J. Sheesley, A. Andersson, and Ö. Gustafsson, Natural abundance  $^{13}\text{C}$  and  $^{14}\text{C}$  analysis of water-soluble organic carbon in atmospheric aerosols, *Anal. Chem.* **82**, 7973–7978 (2010).
- [15] I. Gensch, A. Kiendler-Scharr, and J. Rudolph, Isotope ratio studies of atmospheric organic compounds: Principles, methods, applications and potential, *Int. J. Mass Spectrom.* **365–366**, 206–221 (2014).
- [16] A. Masalaite, R. Holzinger, D. Ceburnis, V. Remeikis, V. Ulevičius, T. Röckmann, and U. Dusek, Sources and atmospheric processing of size segregated aerosol particles revealed by stable carbon isotope ratios and chemical speciation, *Environ. Pollut.* **240**, 286–296 (2018).
- [17] A. Masalaite, R. Holzinger, V. Remeikis, T. Röckmann, and U. Dusek, Characteristics, sources and evolution of fine aerosol (PM<sub>1</sub>) at urban, coastal and forest background sites in Lithuania, *Atmos. Environ.* **148**, 62–76 (2017).
- [18] A. Masalaite, V. Remeikis, A. Garbaras, V. Dudoitis, V. Ulevičius, and D. Ceburnis, Elucidating carbonaceous aerosol sources by the stable carbon  $\delta^{13}\text{C}_{\text{TC}}$  ratio in size-segregated particles, *Atmos. Res.* **158–159**, 1–12 (2015).
- [19] D. Ceburnis, A. Garbaras, S. Szidat, M. Rinaldi, S. Fahrni, N. Perron, L. Wacker, S. Leinert, V. Remeikis, M.C. Facchini, et al., Quantification of the carbonaceous matter origin in submicron marine aerosol by  $^{13}\text{C}$  and  $^{14}\text{C}$  isotope analysis, *Atmos. Chem. Phys.* **11**, 8593–8606 (2011).
- [20] D. Ceburnis, A. Masalaite, J. Ovadnevaite, A. Garbaras, V. Remeikis, W. Maenhaut, M. Claeys, J. Sciare, D. Baisnée, and C.D. O’Dowd, Stable isotopes measurements reveal dual carbon pools contributing to organic matter enrichment in marine aerosol, *Sci. Rep.* **6**, 36675 (2016).
- [21] D. Widory, Nitrogen isotopes: Tracers of origin and processes affecting PM<sub>10</sub> in the atmosphere of Paris, *Atmos. Environ.* **41**, 2382–2390 (2007).

- [22] S.D. Kelly, C. Stein, and T.D. Jickells, Carbon and nitrogen isotopic analysis of atmospheric organic matter, *Atmos. Environ.* **39**, 6007–6011 (2005).
- [23] K. Kawamura, M. Kobayashi, N. Tsubonuma, M. Mochida, T. Watanabe, and M. Lee, Organic and inorganic compositions of marine aerosols from East Asia: Seasonal variations of water-soluble dicarboxylic acids, major ions, total carbon and nitrogen, and stable C and N isotopic composition, *Geochem. Soc. Spec. Pub.* **9**, 243–265 (2004).
- [24] L.A. Martinelli, P.B. Camargo, L.B.L.S. Lara, R.L. Victoria, and P. Artaxo, Stable carbon and nitrogen isotopic composition of bulk aerosol particles in a C4 plant landscape of southeast Brazil, *Atmos. Environ.* **36**, 2427–2432 (2002).
- [25] M. Górka, E. Zwolińska, M. Malkiewicz, D. Lewicka-Szczebak, and M.O. Jędrysek, Carbon and nitrogen isotope analyses coupled with palynological data of PM<sub>10</sub> in Wrocław city (SW Poland) – assessment of anthropogenic impact, *Isot. Environ. Health Stud.* **48**, 327–344 (2012).
- [26] V.C. Turekian, S. Macko, D. Ballentine, R.J. Swap, and M. Garstang, Causes of bulk carbon and nitrogen isotopic fractionations in the products of vegetation burns: Laboratory studies, *Chem. Geol.* **152**, 181–192 (1998).
- [27] S.G. Aggarwal, K. Kawamura, G.S. Umarji, E. Tachibana, R.S. Patil, and P.K. Gupta, Organic and inorganic markers and stable C-, N-isotopic compositions of tropical coastal aerosols from megacity Mumbai: Sources of organic aerosols and atmospheric processing, *Atmos. Chem. Phys.* **13**, 4667–4680 (2013).
- [28] S.G. Yeatman, L.J. Spokes, P.F. Dennis, and T.D. Jickells, Comparisons of aerosol nitrogen isotopic composition at two polluted coastal sites, *Atmos. Environ.* **35**, 1307–1320 (2001).
- [29] S.G. Yeatman, L.J. Spokes, P.F. Dennis, and T.D. Jickells, Can the study of nitrogen isotopic composition in size-segregated aerosol nitrate and ammonium be used to investigate atmospheric processing mechanisms? *Atmos. Environ.* **35**, 1337–1345 (2001).
- [30] S.L. Mkombe, K. Kawamura, E. Tachibana, and P. Fu, Stable carbon and nitrogen isotopic compositions of tropical atmospheric aerosols: sources and contribution from burning of C3 and C4 plants to organic aerosols, *Tellus B* **66**, 20176 (2014).
- [31] K.M. Russell, J.N. Galloway, S.A. Macko, J.L. Moody, and J.R. Scudlark, Sources of nitrogen in wet deposition to the Chesapeake Bay region, *Atmos. Environ.* **32**, 2453–2465 (1998).
- [32] B. Kunwar, K. Kawamura, and C. Zhu, Stable carbon and nitrogen isotopic compositions of ambient aerosols collected from Okinawa Island in the western North Pacific Rim, an outflow region of Asian dusts and pollutants, *Atmos. Environ.* **131**, 243–253 (2016).
- [33] P. Vodička, K. Kawamura, J. Schwarz, B. Kunwar, and V. Ždímal, Seasonal study of stable carbon and nitrogen isotopic composition in fine aerosols at a Central European rural background station, *Atmos. Chem. Phys.* **19**, 3463–3479 (2019).
- [34] A. Garbaras, I. Rimšelytė, K. Kvietkus, and V. Remeikis,  $\delta^{13}\text{C}$  values in size-segregated atmospheric carbonaceous aerosols at a rural site in Lithuania, *Lith. J. Phys.* **49**, 229–236 (2009).
- [35] M. Narukawa, K. Kawamura, N. Takeuchi, and T. Nakajima, Distribution of dicarboxylic acids and carbon isotopic compositions in aerosols from 1997 Indonesian forest fires, *Geophys. Res. Lett.* **26**, 3101–3104 (1999).
- [36] A.F. Stein, R.R. Draxler, G.D. Rolph, B.J.B. Stunder, M.D. Cohen, and F. Ngan, NOAA's HYSPLIT atmospheric transport and dispersion modeling system, *Bull. Am. Meteorol. Soc.* **96**, 2059–2077 (2015).
- [37] Y.J. Yoon, D. Ceburnis, F. Cavalli, O. Jourdan, J.P. Putaud, M.C. Facchini, S. Decesari, S. Fuzzi, K. Sellegri, S.G. Jennings, and C.D. O'Dowd, Seasonal characteristics of the physicochemical properties of North Atlantic marine atmospheric aerosols, *J. Geophys. Res.* **112**, D04206 (2007).
- [38] J. Ovadnevaite, D. Ceburnis, S. Leinert, M. Dall'Osto, M. Canagaratna, S. O'Doherty, H. Berresheim, and C. O'Dowd, Submicron NE Atlantic marine aerosol chemical composition and abundance: Seasonal trends and air mass categorization, *J. Geophys. Res.* **119**, 11, 850–811, 863 (2014).

- [39] A. Milukaitė, K. Kvietkus, and I. Rimšelytė, Organic and elemental carbon in coastal aerosol of the Baltic Sea, *Lith. J. Phys.* **47**(2), 203–210 (2007).
- [40] I. Rimšelytė, J. Ovadnevaitė, D. Čeburnis, K. Kvietkus, and E. Pesliakaitė, Chemical composition and size distribution of fine aerosol particles on the east coast of the Baltic Sea, *Lith. J. Phys.* **47**, 523–529 (2007).
- [41] M. Karl, J.E. Jonson, A. Uppstu, A. Aulinger, M. Prank, M. Sofiev, J.P. Jalkanen, L. Johansson, M. Quante, and V. Matthias, Effects of ship emissions on air quality in the Baltic Sea region simulated with three different chemistry transport models, *Atmos. Chem. Phys.* **19**, 7019–7053 (2019), <https://doi.org/10.5194/acp-19-7019-2019>.
- [42] M. Górka, M.O. Jędrysek, J. Maj, A. Worobiec, A. Buczyńska, E. Stefaniak, A. Krata, R. Van Grieken, A. Zwoździak, I. Sówka, J. Zwoździak, and D. Lewicka-Szczebak, Comparative assessment of air quality in two health resorts using carbon isotopes and palynological analyses, *Atmos. Environ.* **43**, 682–688 (2009).
- [43] M. Górka, M. Rybicki, B.R.T. Simoneit, and L. Marynowski, Determination of multiple organic matter sources in aerosol PM<sub>10</sub> from Wrocław, Poland using molecular and stable carbon isotope compositions, *Atmos. Environ.* **89**, 739–748 (2014).
- [44] A. Mašalaitė, A. Garbaras, and V. Remeikis, Stable isotopes in environmental investigations, *Lith. J. Phys.* **52**, 261–268 (2012).
- [45] L. Jaeglé, L. Steinberger, R. Martin, and K. Chance, Global partitioning of NO<sub>x</sub> sources using satellite observations: Relative roles of fossil fuel combustion, biomass burning and soil emissions, *Faraday Discuss.* **130**, 407–423 (2005).
- [46] Y. Kang, M. Liu, Y. Song, X. Huang, H. Yao, X. Cai, H. Zhang, L. Kang, X. Liu, X. Yan, et al., High-resolution ammonia emissions inventories in China from 1980 to 2012, *Atmos. Chem. Phys.* **16**, 2043–2058 (2016).
- [47] R. Suarez-Bertoa, A.A. Zardini, and C. Astorga, Ammonia exhaust emissions from spark ignition vehicles over the New European Driving Cycle, *Atmos. Environ.* **97**, 43–53 (2014).
- [48] J.N. Cape, Y.S. Tang, N. van Dijk, L. Love, M.A. Sutton, and S.C.F. Palmer, Concentrations of ammonia and nitrogen dioxide at roadside verges, and their contribution to nitrogen deposition, *Environ. Pollut.* **132**, 469–478 (2004).
- [49] C.D. Bray, W. Battye, V.P. Aneja, D.Q. Tong, P. Lee, and Y. Tang, Ammonia emissions from biomass burning in the continental United States, *Atmos. Environ.* **187**, 50–61 (2018).
- [50] Q. Li, J. Jiang, S. Cai, W. Zhou, S. Wang, L. Duan, and J. Hao, Gaseous ammonia emissions from coal and biomass combustion in household stoves with different combustion efficiencies, *Environ. Sci. Technol. Lett.* **3**, 98–103 (2016).
- [51] T.H.E. Heaton, <sup>15</sup>N/<sup>14</sup>N ratios of NO<sub>x</sub> from vehicle engines and coal-fired power stations, *Tellus B*, **42**, 304–307 (1990).
- [52] E.M. Elliott, C. Kendall, S.D. Wankel, D.A. Burns, E.W. Boyer, K. Harlin, D.J. Bain, and T.J. Butler, Nitrogen isotopes as indicators of NO<sub>x</sub> source contributions to atmospheric nitrate deposition across the Midwestern and Northeastern United States, *Environ. Sci. Technol.* **41**, 7661–7667 (2007).
- [53] Y. Chang, Y. Zhang, C. Tian, S. Zhang, X. Ma, F. Cao, X. Liu, W. Zhang, T. Kuhn, and M.F. Lehmann, Nitrogen isotope fractionation during gas-to-particle conversion of NO<sub>x</sub> to NO<sub>3</sub><sup>-</sup> in the atmosphere – implications for isotope-based NO<sub>x</sub> source apportionment, *Atmos. Chem. Phys.* **18**, 11647–11661 (2018).
- [54] M. Ciężka, M. Modelska, M. Górka, A. Trojanowska-Olichwer, and D. Widory, Chemical and isotopic interpretation of major ion compositions from precipitation: A one-year temporal monitoring study in Wrocław, SW Poland, *J. Atmos. Chem.* **73**, 61–80 (2016).

## STABILIJŲ ANGLIES IR AZOTO IZOTOPŲ SANTYKIO TYRIMAI ĮVAIRIAUS DYDŽIO AEROZOLIO DALELĖSE ( $KD_1$ , $KD_{0,056-2,5}$ )

I. Garbarienė<sup>a</sup>, V. Remeikis<sup>b</sup>, A. Mašalaitė<sup>b</sup>, A. Garbaras<sup>b</sup>, T. Petelski<sup>c</sup>, P. Makuch<sup>c</sup>, U. Dusek<sup>d</sup>

<sup>a</sup> *Fizinių ir technologijos mokslų centro Aplinkotyros skyrius, Vilnius, Lietuva*

<sup>b</sup> *Fizinių ir technologijos mokslų centro Branduolinių tyrimų skyrius, Vilnius, Lietuva*

<sup>c</sup> *Okeanologijos instituto Fizinės okeanografijos skyrius, Sopotas, Lenkija*

<sup>d</sup> *Groningeno universiteto Izotopų tyrimų centras, Groningenas, Nyderlandai*

### Santrauka

Pateikiami stabilijų anglies ( $\delta^{13}C$ ) ir azoto ( $\delta^{15}N$ ) izotopų santykio verčių matavimai įvairaus dydžio ( $KD_1$ ,  $KD_{0,056-2,5}$ ) aerozolio dalelėse. Dalelės rinktos kruizo Baltijos jūroje metu 2012 m. lapkričio 9–17 dienomis.

Nustatyta, kad pietvakarinėse oro masėse  $KD_1$  dalelėms būdingos didelės  $\delta^{13}C$  vertės (–26,4 ‰), kurių tikėtinas anglies turinčių aerozolio dalelių šaltinis yra akmens anglies ir dyzelino / benzino deginimas, o mažos  $\delta^{15}N$  (–0,2, 0,8 ‰) vertės parodo skysto kuro deginimo šaltinius (laivų ir autotransporto išmetalai). Bandiniuose, kuriuos renkant vyravo vakarinės oro masės, buvo priešingai – itin mažos  $\delta^{13}C$  (–27,5 ‰) ir

didelės  $\delta^{15}N$  vertės (iki 10 ‰). Tokios  $\delta^{15}N$  vertės labiausiai siejamos su azotinių medžiagų fotocheminiais degradacijos procesais tolimosios pernašos metu, o mažos  $\delta^{13}C$  vertės rodo dyzelino / benzino deginimo šaltinį, kuris šiuo atveju labiausiai siejamas su laivų emisijomis.

Skirtingo dydžio aerozolio dalelių  $\delta^{13}C$  analizė parodė, kad mažiausios  $\delta^{13}C$  vertės buvo registruotos 0,056–0,18  $\mu m$  dydžio dalelėse, o 0,18–2,5  $\mu m$  dalelių dydžio intervale  $\delta^{13}C$  vertės nuosekliai didėjo. Toks kitimas atspindi aerozolio dalelių formavimosi mechanizmus ir šaltinius.